

Is the metallicity of the progenitor of long gamma-ray bursts really low?

Jing-Meng Hao and Ye-Fei Yuan¹

*Key Laboratory for Research in Galaxies and Cosmology CAS,
Department of Astronomy, University of Science and Technology of China,
Hefei, Anhui 230026, China*

ABSTRACT

Observations of long gamma-ray bursts (LGRBs) offer a unique opportunity for probing the cosmic star formation history, although whether or not LGRB rates are biased tracers of star formation rate history is highly debated. Based on an extensive sample of LGRBs compiled by Robertson & Ellis (2012), we analyze various models of star formation rate and the possible effect of the evolution of cosmic metallicity under the assumption that LGRBs tend to occur in low-metallicity galaxies. The models of star formation rate tested in this work include empirical fits from observational data as well as a self-consistent model calculated in the framework of the hierarchical structure formation. Comparing with the observational data, we find a relatively higher metallicity cut of $Z \gtrsim 0.6Z_{\odot}$ for the empirical fits and no metallicity cut for the self-consistent model. These results imply that there is no strong metallicity preference for the host galaxy of LGRBs, in contrast to previous work which suggest a cut of $Z \sim 0.1 - 0.3Z_{\odot}$, and that the inferred dependencies of LGRBs on their host galaxy properties are strongly related to the specific models of star formation rate. Furthermore, a significant fraction of LGRBs occur in small dark matter halos down to $3 \times 10^8 M_{\odot}$ can provide an alternative explanation for the discrepancy between the star formation rate history and LGRB rate history.

Subject headings: galaxies: evolution gamma-ray burst: general

1. Introduction

When reionization was complete and what kind of sources should be responsible for it still remain open questions. The optical depth of electron scattering constrained from the *Wilkinson Microwave Anisotropy Probe* (WMAP) infers that the universe was substantially ionized by $z \sim 10$ (Komatsu et al. 2011), which is somewhat in conflict with the Gunn-Peterson trough in the spectra of high-redshift quasars implying an end to reionization at $z \approx 6$ (Fan et al. 2006). Models which

¹yfyuan@ustc.edu.cn

are consistent with these constraints strongly suggest that reionization is likely to be a much more extended process (Cen 2003; Choudhury & Ferrara 2006; Ilev et al. 2007). In addition, observations of the Ly α forest and the high-redshift galaxies at $z \sim 6 - 10$ infer a photon-starved end to reionization (Bolton & Haehnelt 2007; Oesch et al. 2012). One possibility is that small galaxies forming in the dark matter halos with masses below $\sim 10^9 M_\odot$ produce the bulk of ionizing photons during the epoch of reionization. However, these galaxies are too faint to be detected by the current observational facilities. Even the *James Webb Space Telescope* (JWST) will be incapable of reaching the required sensitivity. Fortunately, long gamma-ray burst (LGRB) observations offer a unique opportunity for probing the history of the high-redshift star formation, unlimited by the faintness of the host galaxy.

As a result of the collapse of massive stars (MacFadyen & Woosley 1999), LGRBs are thought to be well suited to investigate the cosmic star formation rate (CSFR) (Porciani & Madau 2001; Bromm & Loeb 2002; Yüksel et al. 2008; Kistler et al. 2009). Still, this is challenging, because detailed modeling is required to connect the LGRB rate to the CSFR. In this respect, whether or not LGRBs are biased tracers of star formation is highly debated (Daigne et al. 2006; Kistler et al. 2008). Earlier studies (e.g. Kistler et al. 2008) often modeled the relation between the LGRB rate and the CSFR using a redshift dependence quantity which is parameterized as a simple power law, $\Psi(z) \propto (1+z)^\beta$, with $\beta \approx 1.2$. A possible physical explanation for such an enhancement is the cosmic metallicity evolution, because the collapsar model for LGRBs suggests that they can only be produced by stars with metallicity $Z \lesssim 0.1Z_\odot$ (Woosley & Bloom 2006; Langer & Norman 2006; Salvaterra & Chincarini 2007). Observationally, Svensson et al. (2010) and Levesque et al. (2010a) found that LGRBs at $z \lesssim 1$ occur preferentially in relatively low-mass, low-metallicity galaxies. However, the picture is not a simple one: several LGRB hosts with high-metallicity have been found (Graham et al. 2009; Levesque et al. 2010a,b,c), which suggests that a low-metallicity cut-off is unlikely. Compiling a large sample of 46 LGRBs over $0 < z < 6.3$, Savaglio et al. (2009) found that the properties of their host galaxies are those expected for normal star-forming galaxies. Most recently, by analyzing a sample of 22 LGRB hosts with new radio data, Michałowski et al. (2012) have found that the properties of LGRB population are consistent with those of other star-forming galaxies at $z \lesssim 1$, implying that LGRBs trace a large fraction of all star formation. Hence, owing to the limited sample size, the biases of the LGRB hosts in terms of morphology and metallicity are far from being well understood.

In this work we investigate the effect of the evolution of cosmic metallicity placed on the CSFR-LGRB rate connection using an extensive sample of LGRBs compiled by Robertson & Ellis (2012) together with several CSFR models, including empirical models fitted from the observational data as well as a self-consistent model derived from the hierarchical formation scenario using a Press-Schechter-like formalism. This analysis could also be used for a better estimate of the high-redshift CSFR using the LGRB rate as the observational data. Furthermore, this work could contribute to the study of the environments of LGRB host galaxies. This paper is organized as follows. The CSFR and LGRB rate models are explained in Section 2. In Section 3, we compare the predictions

of the different models with the observed cumulative redshift distribution of LGRBs. Conclusions are presented in Section 4.

The cosmological parameters used in this paper are from the WMAP-7 results: $\Omega_m = 0.266$, $\Omega_\Lambda = 0.734$, $\Omega_b = 0.0449$, $h = 0.71$ and $\sigma_8 = 0.801$.

2. LGRB rate

In order to successfully produce a LGRB with a collapsar, the progenitor star has to be sufficiently massive to result in the formation of a central black hole (MacFadyen & Woosley 1999). Then the relationship between the intrinsic LGRB rate and the black hole formation rate can be parameterized as

$$\dot{n}_{\text{GRB}}(z) \propto \Psi(z)\dot{n}_{\text{BH}}(z), \quad (1)$$

where $\dot{n}_{\text{BH}}(z)$ is the black hole formation rate and $\Psi(z)$ is the redshift-dependent LGRB formation efficiency that can be used to model possible biases in the relation between \dot{n}_{BH} and \dot{n}_{GRB} .

2.1. Model for $\Psi(z)$

Kistler et al. (2008) and Robertson & Ellis (2012) found that $\Psi \sim \text{constant}$ was inconsistent with the observational data, implying that there is an enhancement in the LGRB rate by some mechanism at high redshift. As suggested by the collapsar model (MacFadyen & Woosley 1999), the most likely physical explanation for this enhancement is the cosmic metallicity evolution, which has been explored by many authors (Langer & Norman 2006; Salvaterra & Chincarini 2007; Li 2008; Wang & Dai 2009; Butler et al. 2010; Virgili et al. 2011). For instance, Salvaterra & Chincarini (2007) explored a scenario in which LGRBs arise in metal-poor host galaxies, resulting in a metallicity cut of $Z \lesssim 0.1Z_\odot$. Following Langer & Norman (2006) (LN), in the case where LGRBs preferentially occur in galaxies with low-metallicity, the LGRB formation efficiency can be described by an analytical form for the fraction of mass density belonging to metallicity below a given threshold of Z_{th} :

$$\Psi(Z_{\text{th}}, z) = \frac{\hat{\Gamma}[\alpha_1 + 2, (Z_{\text{th}}/Z_\odot)^\beta 10^{0.15\beta z}]}{\Gamma(\alpha_1 + 2)}, \quad (2)$$

where $\hat{\Gamma}$ and Γ are the incomplete and complete gamma functions, $\alpha_1 = -1.16$ is the slope in the Schechter distribution function of galaxy stellar masses (Panter et al. 2004) and $\beta = 2$ is the power-law index of the galaxy mass-metallicity relation. It is worth stressing that this analytical form is based on a Schechter function of galaxy stellar masses from Panter et al. (2004) and the linear bisector fit to the mass-metallicity relation derived by Savaglio et al. (2005), of the form $M/M_* = K(Z/Z_\odot)^\beta$. LN did not address the redshift evolution of the galaxy stellar mass function, and assumed that the average cosmic metallicity simply evolves with redshift accord-

ing to $Z/Z_\odot \propto 10^{-0.15z}$, which is from the metallicity measurements of emission-line galaxies by Kewley & Kobulnicky (2005). The validity of these simplifications needs to be examined.

Following Li (2008), we estimate the redshift evolution of the average metallicity below. Given the scaling $12 + \log(\text{O}/\text{H}) = \log(Z/Z_\odot) + 8.69$ (Allende Prieto et al. 2001), the redshift-dependent mass-metallicity relation derived by Savaglio et al. (2005) can be written as

$$\begin{aligned} \log(Z/Z_\odot) = & -16.2803 + 2.5315 \log M \\ & -0.09649 \log^2 M \\ & +5.1733 \log t_{\text{H}} - 0.3944 \log^2 t_{\text{H}} \\ & -0.403 \log t_{\text{H}} \log M, \end{aligned} \quad (3)$$

where t_{H} is the Hubble time in units of Gyr and M is the galaxy stellar mass in units of M_\odot . Equation (3) then can be used to calculate the average metallicity which is defined by averaging over the stellar mass

$$\left\langle \frac{Z}{Z_\odot} \right\rangle \equiv \frac{\int_0^\infty Z(M, z) M \Phi(M) dM}{Z_\odot \int_0^\infty M \Phi(M) dM}. \quad (4)$$

By adopting a redshift evolving stellar mass function from Drory & Alvarez (2008),

$$\begin{aligned} \Phi(M, z) dM &= \Phi_* \left(\frac{M}{M_*} \right)^\gamma \exp\left(-\frac{M}{M_*}\right) \frac{dM}{M_*}, \\ \Phi_* &\approx 0.003(1+z)^{-1.07} \text{Mpc}^{-3} \text{dex}^{-1} \\ \log M_*(z) &\approx 11.35 - 0.22 \ln(1+z) \\ \gamma(z) &\approx -1.3, \end{aligned} \quad (5)$$

$\langle Z/Z_\odot \rangle$ is calculated and shown in Fig. 1, with comparison to the measurements from Kewley & Kobulnicky (2005). The result of $\langle Z/Z_\odot \rangle$ with the non-evolving stellar mass function from Panter et al. (2004) is also shown in Fig. 1. As can be seen, the redshift evolution of the metallicity according to $Z/Z_\odot \propto 10^{-0.15z}$ evolves more rapidly to lower metallicity with increasing redshift than that of $\langle Z/Z_\odot \rangle$ with both the evolving and the non-evolving stellar mass function. This is because that the contribution to $\langle Z/Z_\odot \rangle$ is dominated by galaxies with stellar masses around $M_* \sim 10^{11}$ while faster evolution and lower metallicity are primarily due to galaxies with smaller stellar masses (Savaglio et al. 2005; Li 2008). However, due to the limited number of LGRBs with measured redshifts and many uncertain biases, such as their selection effects, evolving luminosity function, the evolving stellar initial mass function (IMF), for our purpose, it is enough to adopt the analytical form of LN in this paper.

Other than LN, Robertson & Ellis (2012) extended the model of Kocevski et al. (2009) to calculate $\Psi(z)$ from the fraction of star formation occurring below some metallicity cut. They found that star formation occurring in galaxies with metallicity below the value $12 + \log[\text{O}/\text{H}]_{\text{crit}} \approx 8.7$, which corresponds to $Z \sim 0.6 - 1.0Z_\odot$ depending on the adopted metallicity scale and solar abundance value (Modjaz et al. 2008), tracks the LGRB rate with high consistency and parameterized

it as:

$$\Psi_{\text{fit}}(z) = 0.5454 + (1 - 0.5454) \times [\text{erf}(0.324675z)]^{1.45}. \quad (6)$$

In Fig. 2, we show a comparison of equation (2) with different values in metallicity cut ($Z_{\text{th}} = 0.1 - 0.6Z_{\odot}$) and the parameterized best-fit from Robertson & Ellis (2012). As can be seen, the best-fit of Robertson & Ellis (2012) is similar to the $Z = 0.6Z_{\odot}$ case of LN.

2.2. The CSFR models

The black hole formation rate $\dot{n}_{\text{BH}}(z)$ is calculated by

$$\dot{n}_{\text{BH}}(t) = \int_{m_{\text{BH}}}^{m_{\text{up}}} \Phi(m) \dot{\rho}_*(t - \tau_m) dm. \quad (7)$$

where the lower limit of the integral, m_{BH} , corresponds to the minimum mass of a star that could collapse to a BH, which we set to be $25M_{\odot}$ (Bromm & Loeb 2002), $\Phi(m)$ is the stellar IMF and $\dot{\rho}_*(t - \tau_m)$ represents the CSFR at the retarded time ($t - \tau_m$), where τ_m is the lifetime of a star of mass m .

We consider that the IMF follows the Salpeter (1955) form $\Phi(m) = Am^{-2.35}$ and this function is normalized as $\int_{m_{\text{inf}}}^{m_{\text{up}}} Am^{-2.35} m dm = 1$, where we take $m_{\text{inf}} = 0.1 M_{\odot}$ and $m_{\text{up}} = 140$ for lower and upper mass limits respectively.

The stellar lifetime τ_m as a function of mass m is given by the fit of Scalo (1986) and Copi (1997):

$$\log_{10}(\tau_m) = 10.0 - 3.6 \log_{10} \left(\frac{M}{M_{\odot}} \right) + \left[\log_{10} \left(\frac{M}{M_{\odot}} \right) \right]^2. \quad (8)$$

For CSFR $\dot{\rho}_*$, there are many forms available in the literature. Kistler et al. (2008, 2009) and Robertson & Ellis (2012) adopted the piecewise-linear model of Hopkins & Beacom (2006), which provides a good statistical fit to the available star formation density data. However, it should be stressed that the empirical fit will obviously vary depending on the functional form as well as the observational data used. As a comparison, we also consider the model of Cole et al. (2001), which use the parametric form:

$$\dot{\rho}_* = \frac{(a + bz)h}{1 + (z/c)^d}, \quad (9)$$

where $h = 0.7$, $a = 0.017$, $b = 0.13$, $c = 3.3$ and $d = 5.3$ (Hopkins & Beacom 2006).

In addition, we utilize a self-consistent model of Pereira & Miranda (2010). In the framework of hierarchical structure formation using a Press-Schechter-like formalism, Pereira & Miranda (2010) obtained the CSFR by means of solving the equations governing the total gas density taking into account the baryon accretion rate and the lifetime of the stars formed in the dark matter halos. We show two model predictions with different assumptions on the threshold dark matter halo mass

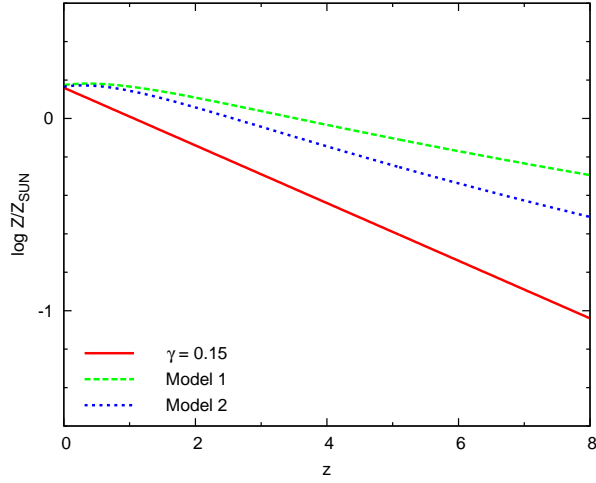


Fig. 1.— Cosmic average metallicity as a function of redshift z . The solid line is the evolution of the metallicity according to $Z/Z_{\odot} \propto 10^{-0.15z}$. The dashed line and dotted line are the average metallicities calculated by adopting the redshift-dependent mass-metallicity relation of Savaglio et al. (2005), with the non-evolving (Model 1) and evolving (Model 2) stellar mass function, respectively.

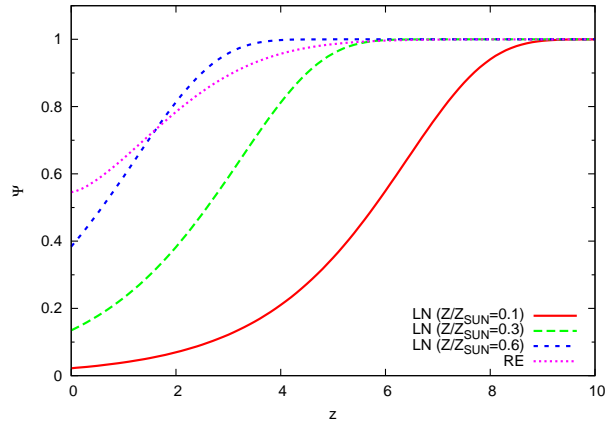


Fig. 2.— Fraction of the density of the stellar mass in galaxies with metallicities below a certain threshold of Z/Z_{\odot} as a function of redshift z . These results are from Langer & Norman (2006)(LN). The metallicity cuts are taken to be $Z_{\text{th}} = 0.1$ (solid line), 0.3 (dashed line), 0.6 (short-dashed line), respectively. A parameterized fit from Robertson & Ellis (2012) (RE) is also shown in dotted line for comparison.

below which galaxy formation is suppressed: $M_{\text{min}} = 3 \times 10^8 M_{\odot}$ and $M_{\text{min}} = 3 \times 10^9 M_{\odot}$. The lower value assumes the star formation proceeds in dark matter halos down to the limit of HI cooling ($T_{\text{vir}} \sim 2 \times 10^4 \text{ K}$), while the higher value corresponds to a fit to the observed high redshift CSFR, which successfully reproduces the CSFR from $z = 5$ to $z = 8$.

All these different CSFRs are summarized in Fig. 3, compared to data from Hopkins (2004, 2007) and Li (2008). As can be seen, all of these models are similar and have good agreement with observational data at redshift $z < 4$. At high redshifts, the Pereira & Miranda (2010) CSFR remains much flatter than the two empirical fits from Hopkins & Beacom (2006) and Cole et al. (2001), which are already beginning to drop exponentially.

3. Comparison with the observational data

In order to compare with observations, we calculate the expected cumulative redshift distribution of LGRBs as

$$N(< z) = A \int_0^z \Psi(z) \dot{n}_{\text{BH}}(z) \frac{dV}{dz} \frac{dz}{1+z}, \quad (10)$$

where A is a constant that depends on the observing time, sky coverage, the survey flux limit and so on. dV/dz is the comoving volume element per unit redshift, given by

$$\frac{dV}{dz} = \frac{4\pi c d_L^2}{1+z} \left| \frac{dt}{dz} \right|, \quad (11)$$

where d_L is the luminosity distance and dt/dz is given by (Pereira & Miranda 2010)

$$\frac{dt}{dz} = \frac{9.78 h^{-1} \text{ Gyr}}{(1+z) \sqrt{\Omega_{\Lambda} + \Omega_{\text{m}}(1+z)^3}}. \quad (12)$$

The constant A can be removed by simply normalizing the cumulative redshift of GRBs to $N(0, z_{\text{max}})$, as

$$N(< z | z_{\text{max}}) = \frac{N(0, z)}{N(0, z_{\text{max}})}. \quad (13)$$

Our LGRB sample is taken from Robertson & Ellis (2012), which is consist of 162 long GRBs with measured redshifts or redshift limits. Robertson & Ellis (2012) chose the sample from Butler et al. (2007), Perley et al. (2009), Butler et al. (2010), Sakamoto et al. (2011), Greiner et al. (2011) and Krühler et al. (2011), including only LGRBs occurring before the end of the Second *Swift* BAT GRB Catalog. To remove the influence of the *Swift* threshold owing to which low luminosity bursts could not have been seen at higher z , as in Kistler et al. (2008) and Robertson & Ellis (2012), we use bursts only with isotropic-equivalent luminosities $L_{\text{iso}} > 10^{51} \text{ ergs s}^{-1}$ which is computed by

$$L_{\text{iso}} = \frac{E_{\text{iso}}}{T_{90}/(1+z)}, \quad (14)$$

where E_{iso} is the isotropic-equivalent energy and T_{90} is the time interval containing 90% of the prompt emission. This culling leaves us 87 GRBs over $0 < z < 4$. For more details on the burst sample, see Robertson & Ellis (2012).

Fig. 4 shows the comparison between the cumulative redshift distribution of observed LGRBs and the expectations $N(< z | z_{\text{max}} = 4)$ with the adoption of the Hopkins & Beacom (2006) CSFR model, for three choices of the metallicity cut and the parameterized best-fit of Robertson & Ellis (2012). We then use the one-sample Kolmogorov-Smirnov (K-S) test to evaluate the consistency between the observed and expected LGRB redshift distributions. In agreement with previous studies (Kistler et al. 2008; Robertson & Ellis 2012), the model with no metallicity cut shows little consistency with the observations, with $P \approx 0.1$. However, in contrast to previous studies that suggest a metallicity cut of $Z_{\text{th}} \lesssim 0.3Z_{\odot}$ (Woosley & Heger 2006; Langer & Norman 2006; Salvaterra & Chincarini 2007; Li 2008; Campisi et al. 2010), the model with a cut of $Z_{\text{th}} = 0.3Z_{\odot}$ shows little consistency with the data. Only the intermediate model adopting the value of $Z_{\text{th}} = 0.6Z_{\odot}$ shows high consistency with the data, similar to the model from the best-fit of Robertson & Ellis (2012). On the other hand, when assuming the Cole et al. (2001) model for the star formation rate, even the model with no metallicity cut is fully consistent with the data at the probability level of 0.78 (Fig. 5). The K-S test gives the probability 99% of a more relaxed cut of $Z_{\text{th}} = 0.9Z_{\odot}$. Note that this higher cut is also more consistent with recent studies of the LGRB host galaxies (Graham et al. 2009; Levesque et al. 2010a,b; Michałowski et al. 2012). The test statistics and probability for the relevant models are summarized in Table 1.

We now consider the self-consistent CSFR model of Pereira & Miranda (2010). Fig. 6 shows a comparison with the cumulative redshift distribution of the 62 LGRBs with $z < 5$ and $L > 3 \times 10^{51} \text{ erg s}^{-1}$, normalized over the redshift range $0 < z < 5$. As can be seen, provided that the star formation proceeds in dark matter halos down to the limit of HI cooling ($T_{\text{vir}} \sim 2 \times 10^4 \text{ K}$ and $M_{\text{DM}} \sim 3 \times 10^8 M_{\odot}$), the calculated LGRB redshift distribution $N(< z | z_{\text{max}} = 5)$ fits the observational data very well even without considering the extra evolution effect of metallicity ($P \approx 0.96$), implying that LGRBs are occurring in any type of galaxy. This result also implies an alternative explanation for the CSFR-LGRB rate discrepancy, i.e., there is significant star formation in faint galaxies, as suggested by Trenti et al. (2012). To illustrate this, we utilize this CSFR model to calculate the LGRB distributions for different threshold masses of dark matter halos. The results are shown in Fig. 7 and demonstrate that the LGRB redshift distribution is consistent with a threshold halo mass of $M_{\text{min}} = 3 \times 10^8 M_{\odot}$ at 96% level (and $M_{\text{min}} = 3 \times 10^9 M_{\odot}$ at 39% level). This is also in agreement with what is found by Muñoz & Loeb (2011), in which the minimum mass halo capable of hosting galaxies is suggested to be around $2.5 \times 10^9 M_{\odot}$.

4. Conclusion

The association of LGRBs with the death of massive stars has presented a unique opportunity for probing the history of star formation at high redshift. In this case, the manner in which how

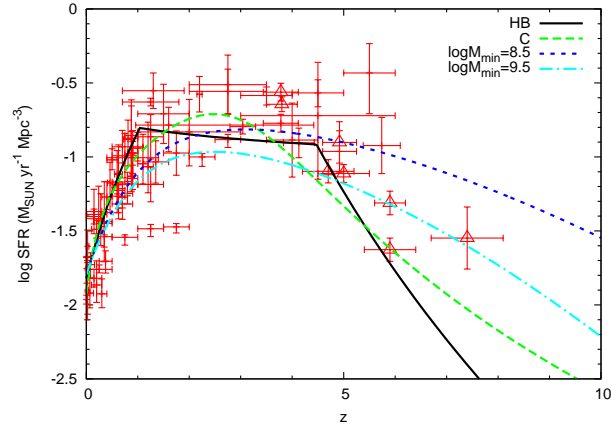


Fig. 3.— Cosmic Star Formation Rate (CSFR) versus redshift z . The solid line represents the empirical fit of Hopkins & Beacom (2006) (HB) and the dashed line corresponds the empirical fit of Cole et al. (2001) (C). The short-dashed line and dot-dashed line represent the model of Pereira & Miranda (2010) with a threshold mass: $\log M_{\min} = 8.5$ and $\log M_{\min} = 9.5$, respectively. The observational data is taken from Hopkins (2004, 2007) and Li (2008).

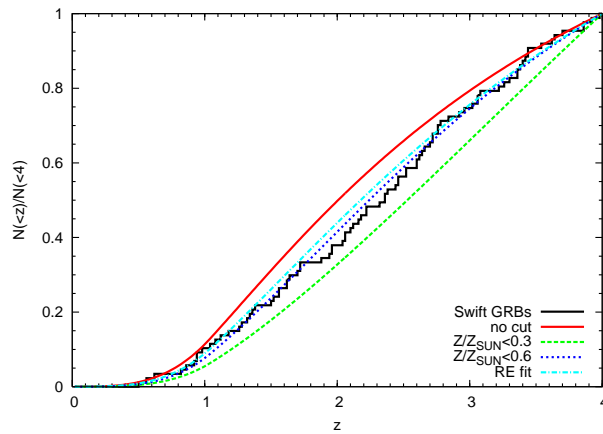


Fig. 4.— Cumulative redshift distribution of LGRBs with $z < 4$ and $L_{\text{iso}} > 10^{51} \text{ergs}^{-1}$. The observational sample with 87 LGRBs are from Robertson & Ellis (2012). The model distributions are calculated assuming the Hopkins & Beacom (2006) CSFR model, for three choices of the metallicity cuts given by Equation (2) and the parameterized best-fit from Robertson & Ellis (2012).

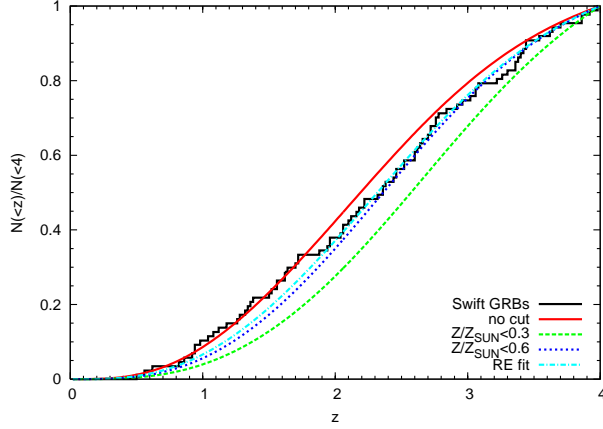


Fig. 5.— Same as Fig. 4, but the star formation rate is based on the model of Cole et al. (2001)

Table 1: Statistical tests of the models of CSFR for a variety of metallicity cuts

CSFR model	Metal cut (Z/Z_{\odot})	K-S test
		D-stat, Prob
HB ¹	no cut	0.1289, 0.1021
HB	0.3	0.1309, 0.0930
HB	0.6	0.0465, 0.9903
HB	RE fit	0.0705, 0.7652
C ²	no cut	0.0696, 0.7793
C	0.6	0.0923, 0.4305
C	0.9	0.0537, 0.9587
C	RE fit	0.0714, 0.7512
PM ³	no cut	0.0620, 0.9663
PM	0.3	0.2218, 0.0036
PM	0.6	0.1107, 0.4120

¹ Hopkins & Beacom (2006)

² Cole et al. (2001)

³ Pereira & Miranda (2010)

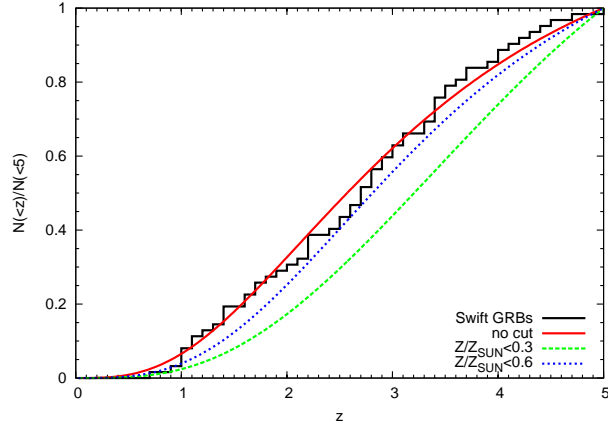


Fig. 6.— Cumulative redshift distribution of LGRBs with $z < 5$ and $L_{\text{iso}} > 3 \times 10^{51} \text{ergs}^{-1}$. The observational sample with 62 LGRBs are from Robertson & Ellis (2012), and the theoretical distributions $N(< z|z_{\text{max}} = 5)$ are based on the self-consistent star formation rate model of Pereira & Miranda (2010) with different metallicity cuts. The threshold mass of dark matter halo is $\log M_{\text{min}} = 8.5$.

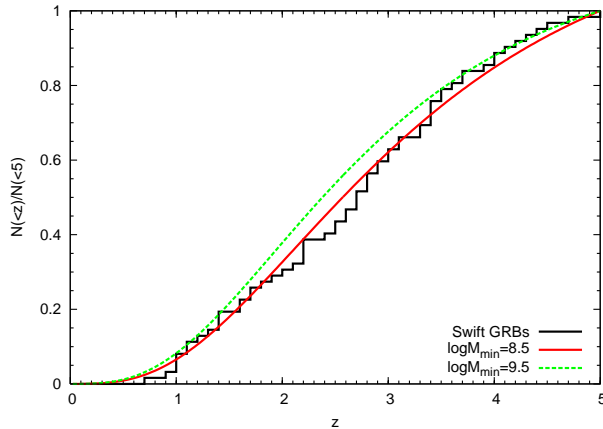


Fig. 7.— Theoretical distributions of LGRBs in the CSFR model of Pereira & Miranda (2010) with two threshold masses ($\log M_{\text{min}} = 8.5$ and $\log M_{\text{min}} = 9.5$).

the LGRB rate traces the CSFR should to be known. In this work, we have investigated the idea that LGRBs as biased tracers of the CSFR occur preferentially in galaxies with low-metallicity. We have tested various CSFR models together with the metallicity considerations of Langer & Norman (2006) using the constraints from newly discovered bursts.

Comparing with the cumulative redshift distribution of luminous ($L_{\text{iso}} > 10^{51} \text{ergs s}^{-1}$) *Swift* LGRBs compiled by Robertson & Ellis (2012) over $0 < z < 4$, we find a relatively higher metallicity cut of $Z_{\text{th}} = 0.6 - 0.9Z_{\odot}$ for both star formation rate models of Hopkins & Beacom (2006) and Cole et al. (2001), in contrast to previous studies which suggest a strong metallicity cut of $\sim 0.1 - 0.3Z_{\odot}$ (Salvaterra & Chincarini 2007; Campisi et al. 2010; Virgili et al. 2011). Especially when considering a self-consistent star formation model of Pereira & Miranda (2010) that takes into account a hierarchical structure formation scenario using a Press-Schechter-like formalism, the calculated expectations show strong consistency with the observational data over $0 < z < 5$, requiring no metallicity cut at all. These results imply that LGRBs trace a large fraction of all star formation with no preference on the properties of their host galaxies, and are therefore less biased indicators than previously thought, which is consistent with recent studies on LGRB hosts (Michałowski et al. 2012; Elliott et al. 2012). Therefore, we conclude that LGRBs populate all types of star-forming galaxies, with no strong metallicity preference. Using the self-consistent CSFR model, we also find that the scenario that a significant fraction of LGRBs occur in small dark matter halos down to $3 \times 10^8 M_{\odot}$ can provide an alternative explanation for the discrepancy between the CSFR history and LGRB rate history. Our results also show that the inferred dependencies of LGRBs on their host galaxy properties are strongly related to the specific CSFR model one adopts, suggesting that detailed observations of individual LGRB host galaxies are essential to provide a better understanding of the metallicity cut for LGRB production. If numbers of similar observations are confirmed, it could mean that the key role that metallicity plays in the production of LGRBs, which is suggested by the traditional collapsar model, needs reconsideration in future studies or it may need alternative progenitor pathways that do not necessarily require a low-metallicity environment.

We thank the anonymous referee for her/his useful suggestions which are helpful for improving the manuscript. This work is partially supported by National Basic Research Program of China (2009CB824800, 2012CB821800), the National Natural Science Foundation (11073020, 11133005, 11233003), and the Fundamental Research Funds for the Central Universities (WK2030220004).

REFERENCES

- Allende Prieto, C., Lambert, D. L., & Asplund, M. 2001, *ApJ*, 556, L63
- Bolton, J. S., & Haehnelt, M. G. 2007, *MNRAS*, 382, 325
- Bromm, V., & Loeb, A. 2002, *ApJ*, 575, 111

- Butler, N. R., Bloom, J. S., & Poznanski, D. 2010, *ApJ*, 711, 495
- Butler, N. R., Kocevski, D., Bloom, J. S., & Curtis, J. L. 2007, *ApJ*, 671, 656
- Campisi, M. A., Li, L.-X., & Jakobsson, P. 2010, *MNRAS*, 407, 1972
- Cen, R. 2003, *ApJ*, 591, 12
- Choudhury, T. R., & Ferrara, A. 2006, *MNRAS*, 371, L55
- Cole, S., Norberg, P., Baugh, C. M., et al. 2001, *MNRAS*, 326, 255
- Copi, C. J. 1997, *ApJ*, 487, 704
- Daigne, F., Rossi, E. M., & Mochkovitch, R. 2006, *MNRAS*, 372, 1034
- Drory, N., & Alvarez, M. 2008, *ApJ*, 680, 41
- Elliott, J., Greiner, J., Khochfar, S., et al. 2012, *A&A*, 539, A113
- Fan, X., Carilli, C. L., & Keating, B. 2006, *ARA&A*, 44, 415
- Graham, J. F., Fruchter, A. S., Kewley, L. J., et al. 2009, in *American Institute of Physics Conference Series*, Vol. 1133, *American Institute of Physics Conference Series*, ed. C. Meegan, C. Kouveliotou, & N. Gehrels, 269–272
- Greiner, J., Krühler, T., Klose, S., et al. 2011, *A&A*, 526, A30
- Hopkins, A. M. 2004, *ApJ*, 615, 209
- . 2007, *ApJ*, 654, 1175
- Hopkins, A. M., & Beacom, J. F. 2006, *ApJ*, 651, 142
- Iliev, I. T., Mellema, G., Shapiro, P. R., & Pen, U.-L. 2007, *MNRAS*, 376, 534
- Kewley, L., & Kobulnicky, H. A. 2005, in *Astrophysics and Space Science Library*, Vol. 329, *Starbursts: From 30 Doradus to Lyman Break Galaxies*, ed. R. de Grijs & R. M. González Delgado, 307
- Kistler, M. D., Yüksel, H., Beacom, J. F., Hopkins, A. M., & Wyithe, J. S. B. 2009, *ApJ*, 705, L104
- Kistler, M. D., Yüksel, H., Beacom, J. F., & Stanek, K. Z. 2008, *ApJ*, 673, L119
- Kocevski, D., West, A. A., & Modjaz, M. 2009, *ApJ*, 702, 377
- Komatsu, E., Smith, K. M., Dunkley, J., et al. 2011, *ApJS*, 192, 18
- Krühler, T., Greiner, J., Schady, P., et al. 2011, *A&A*, 534, A108

- Langer, N., & Norman, C. A. 2006, *ApJ*, 638, L63
- Levesque, E. M., Kewley, L. J., Berger, E., & Zahid, H. J. 2010a, *AJ*, 140, 1557
- Levesque, E. M., Kewley, L. J., Graham, J. F., & Fruchter, A. S. 2010b, *ApJ*, 712, L26
- Levesque, E. M., Soderberg, A. M., Kewley, L. J., & Berger, E. 2010c, *ApJ*, 725, 1337
- Li, L.-X. 2008, *MNRAS*, 388, 1487
- MacFadyen, A. I., & Woosley, S. E. 1999, *ApJ*, 524, 262
- Michałowski, M. J., Kamble, A., Hjorth, J., et al. 2012, *ApJ*, 755, 85
- Modjaz, M., Kewley, L., Kirshner, R. P., et al. 2008, *AJ*, 135, 1136
- Muñoz, J. A., & Loeb, A. 2011, *ApJ*, 729, 99
- Oesch, P. A., Bouwens, R. J., Illingworth, G. D., et al. 2012, *ApJ*, 745, 110
- Panther, B., Heavens, A. F., & Jimenez, R. 2004, *MNRAS*, 355, 764
- Pereira, E. S., & Miranda, O. D. 2010, *MNRAS*, 401, 1924
- Perley, D. A., Cenko, S. B., Bloom, J. S., et al. 2009, *AJ*, 138, 1690
- Porciani, C., & Madau, P. 2001, *ApJ*, 548, 522
- Robertson, B. E., & Ellis, R. S. 2012, *ApJ*, 744, 95
- Sakamoto, T., Barthelmy, S. D., Baumgartner, W. H., et al. 2011, *ApJS*, 195, 2
- Salpeter, E. E. 1955, *ApJ*, 121, 161
- Salvaterra, R., & Chincarini, G. 2007, *ApJ*, 656, L49
- Savaglio, S., Glazebrook, K., & Le Borgne, D. 2009, *ApJ*, 691, 182
- Savaglio, S., Glazebrook, K., Le Borgne, D., et al. 2005, *ApJ*, 635, 260
- Scalo, J. M. 1986, *Fund. Cosmic Phys.*, 11, 1
- Svensson, K. M., Levan, A. J., Tanvir, N. R., Fruchter, A. S., & Strolger, L.-G. 2010, *MNRAS*, 405, 57
- Trenti, M., Perna, R., Levesque, E. M., Shull, J. M., & Stocke, J. T. 2012, *ApJ*, 749, L38
- Virgili, F. J., Zhang, B., Nagamine, K., & Choi, J.-H. 2011, *MNRAS*, 417, 3025
- Wang, F. Y., & Dai, Z. G. 2009, *MNRAS*, 400, L10

Woosley, S. E., & Bloom, J. S. 2006, *ARA&A*, 44, 507

Woosley, S. E., & Heger, A. 2006, *ApJ*, 637, 914

Yüksel, H., Kistler, M. D., Beacom, J. F., & Hopkins, A. M. 2008, *ApJ*, 683, L5